



Self-assembly of a cavitand-based heteronuclear coordination cage

Francesca Gruppi^a, Francesca Boccini^a, Lisa Elviri^b, Enrico Dalcanale^{a,*}

^a Dipartimento di Chimica Organica ed Industriale and Unità INSTM, Università di Parma, Viale Usberti 17/A, 43100 Parma, Italy

^b Dipartimento di Chimica Generale ed Inorganica, Chimica Analitica, Chimica Fisica, Università di Parma, Viale Usberti 17/A, 43100 Parma, Italy

ARTICLE INFO

Article history:

Received 9 September 2008

Accepted 5 November 2008

Available online 24 March 2009

In memory of Dmitry M. Rudkevich

Keywords:

Heteronuclear coordination cages

Cavitands

Self-assembly

ABSTRACT

A new self-assembly protocol leading to the formation of heteronuclear coordination cage **10** is reported. Reaction of tetradentate cavitand ligand **1**, bearing one ethynylpyridine and three benzonitriles at the apical positions, with Pt(dppp)OTf₂ and Pd(dppp)OTf₂ in a 1:3 ratio yields **10** as the thermodynamic product. Under the same conditions, the self-assembly of **1** with either Pt or Pd metal precursors gives a mixture of isomeric homonuclear cages **8a–c** or **9a–c**, respectively.

© 2009 Elsevier Ltd. All rights reserved.

1. Introduction

The self-assembly of coordination cages has reached a high level of sophistication with regard to ligand design and selection of metal precursors.¹ As a result, the shape, dimensions, and polarity of the internal cavity can be engineered, allowing for inclusion of diverse neutral² and charged guests³ in different solvents. The compartmentalization of these guests imparts a wide spectrum of useful properties, including catalysis,^{4,5} storage,⁶ and the stabilization of labile chemical species.⁷

A missing feature in these self-assembly protocols is the differentiation in metal/ligand reactivity necessary for the generation of heteronuclear coordination cages. As a first step in this direction, Kobayashi and co-workers reported the preparation of heterocages, coordination cages featuring two different ligands.^{8,9} Two complementary tetradentate cavitand ligands were prepared, each bearing four identical coordination groups at the apical positions, either nitriles¹⁰ or pyridines.⁸ By utilizing the two cavitand's different coordination ability, they devised self-assembly conditions leading to the formation of either homonuclear Pd or Pt heterocages as the dominant product under kinetic control.

The formation of heteronuclear cages introduces a further level of complexity, where at least two metal/ligand couples must undergo self-sorting during the assembly procedure. For instance, the choice of coordinating ligands and metal precursors must be well-defined

to differentiate their cross-reactivity. At the same time, the different coordinating groups must be inserted at a single macrocyclic ligand site and organized in a precise relative spatial orientation.

In this paper we report a thermodynamically controlled self-assembly protocol leading to the exclusive formation of a Pd/Pt heteronuclear cage. The protocol is based on a tetradentate cavitand ligand functionalized with three nitriles and one pyridine at the upper rim.

2. Result and discussion

2.1. Synthesis of cavitand **1**

The tetradentate cavitand ligand **1**, designed for the self-assembly of heteronuclear coordination cages, presents three benzonitrile and one ethynylpyridine ligands, all of which inserted at the apical positions of a methylene-bridged cavitand (Fig. 1). The choice of these different ligands at the upper rim of the cavitand was dictated by two factors: (i) their different coordination ability toward transition metals like Pt or Pd and (ii) their almost identical distance and orientation with respect to the cavitand scaffold, in order to avoid mismatch during self-assembly.¹¹

The four-step synthesis of cavitand **1** is presented in Scheme 1. Resorcinarene **2**, equipped with hexyl feet to assure solubility in organic solvents, was synthesized according to published procedure.¹² Tetraiodo-resorcinarene **3** was obtained from the reaction of resorcinarene **2** with iodine in the presence of sodium hydrogencarbonate.¹³ The reaction was carried out at room temperature in a 1:1 mixture of water and diethyl ether. The desired product

* Corresponding author. Tel.: +39 0521 905 463; fax: +39 0521 905 472.

E-mail address: enrico.dalcanale@unipr.it (E. Dalcanale).

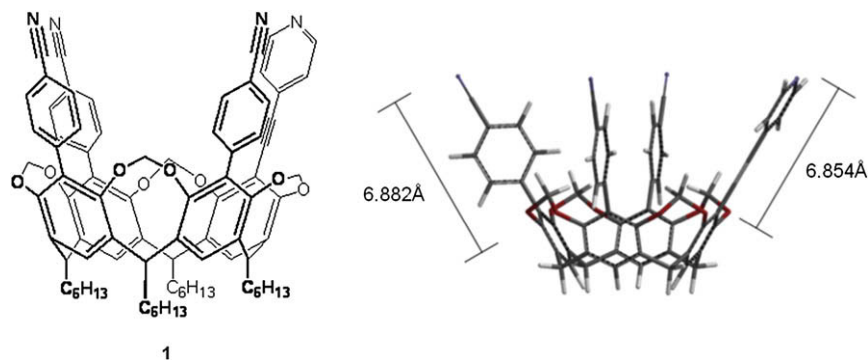


Figure 1. Structure of cavitant **1** and Spartan modeling showing the distance and orientation of the two ligands with respect to the cavitant scaffold.

precipitated in pure form at the water–organic interface (36% yield). Reaction of **3** with CH_2ClBr in a Schlenk apparatus¹⁴ afforded methylene-bridged tetraiodo-cavitant **4** in very high yield (88%). Sonogashira coupling on **4** gave monoethynylpyridine derivative **5**, which underwent a multiple Suzuki coupling to give the desired cavitant **1**.

2.2. Self-assembly of cage 8

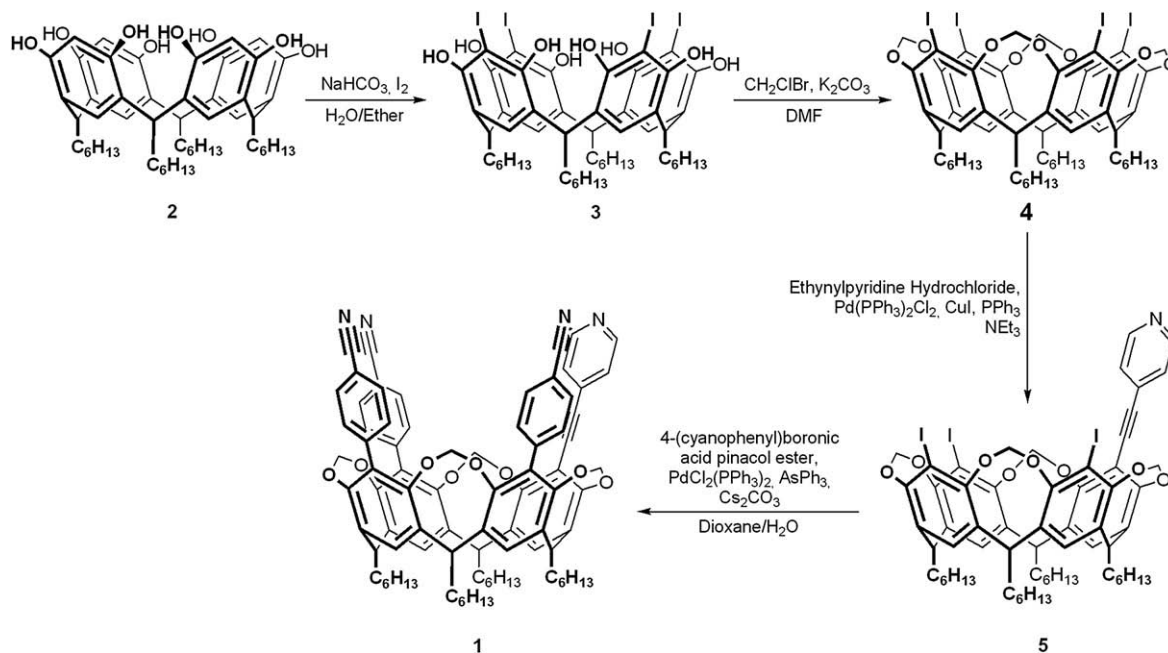
We first explored the complexation behavior of tetradentate ligand **1** against a single metal precursor of general structure $\text{M}(\text{dppp})\text{OTf}_2$, where dppp is 1,3-bis(diphenylphosphino)propane. A stepwise protocol, depicted in Scheme 2, was devised for both $\text{Pt}(\text{dppp})\text{OTf}_2$ and $\text{Pd}(\text{dppp})\text{OTf}_2$.

Metal complex (0.5 equiv) was added to a 5 mM solution of cavitant **1** in a mixture of CD_2Cl_2 (400 μL) and CD_3NO_2 (100 μL). CD_3NO_2 was added to accelerate the ligand exchange¹⁵ in order to reach the thermodynamic equilibrium in reasonable time. Subsequently, the remaining 1.5 equiv of metal precursor was added to the solution. ^1H and ^{31}P NMR spectra were used to track the self-assembly process. The cages were identified by ESI mass spectrometry.

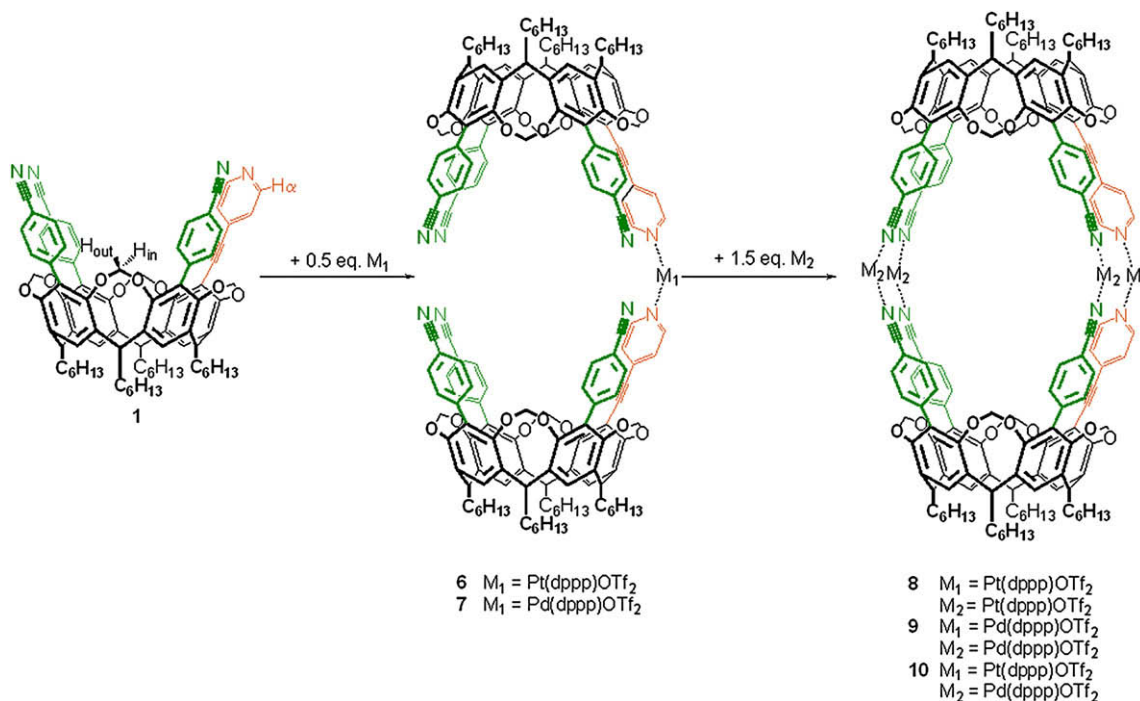
The addition of further 1.5 equiv of $\text{Pt}(\text{dppp})\text{OTf}_2$ led to complete closure of the cage, as confirmed by ESI MS. The mass spectrum evidenced a prominent signal at 2938.2 m/z , corresponding to the doubly charged cage ion. However, as shown in Figure 2c and d, two NMR signals corresponding to the ethynylpyridine α -H were present at 8.81 and 8.61 ppm. The intensity ratio of the two peaks was 1:1 immediately after the addition of the metal complex, but became 1:3 after 48 h and remained stable thereafter. Moreover, a splitting of the signals corresponding to H_{in} and H_{out} of the methylene bridges was observed. After completion of the reaction, the ^{31}P NMR spectrum presented a second signal at -10.02 ppm, in addition to -15.60 ppm peak in a 3:1 ratio.

Taken together these observations indicate the presence of more than one isomeric cage in solution. As shown in Figure 3, in addition to the structure in which the two ethynylpyridines are coordinated to the same metal center (**8a**), the formation of two other isomers is conceivable. In such isomers (**8b** and **8c**), one $\text{Pt}(\text{dppp})\text{OTf}_2$ complex is coordinated to an ethynylpyridine and a benzonitrile ligand. In the case of **8b**, 2 equiv structures are possible, obtained by rotating one cavitant ligand in **8a** by $\pm 90^\circ$.

As reported by Kobayashi and co-workers,⁸ the ^1H NMR signal corresponding to the α -H protons of the ethynylpyridine ligand is



Scheme 1. Synthesis of tetradentate cavitant ligand **1**.



Scheme 2. Stepwise self-assembly protocol.

slightly upfield shifted for the EtPy–Pt–NCPH system compared to the EtPy–Pt–EtPy system. Therefore, the new signal detected at 8.61 ppm is consistent with cages **8b** and **8c**, which cannot be differentiated by NMR.

Kobayashi and co-workers demonstrated that heterocages can be formed as kinetic products, whereas the thermodynamic products were always the homocages of ethynylpyridine and benzonitrile.⁸ The driving force of the self-assembly was the higher coordination ability of the ethynylpyridine ligand. The homocage composed by two identical tetraethynylpyridine cavitant was the thermodynamically favored product.

However, in our system all isomeric cages require the formation of the same set of coordinative bonds, namely two EtPy–Pt and six PhCN–Pt bonds. There is no energy gain in binding two

ethynylpyridines to the same metal center, as opposed to binding them to two different Pt complexes. Therefore, the three possible structures are energetically equivalent, as demonstrated by the 3:1 observed **8b,c/8a** ratio.

2.3. Self-assembly of cage 9

The same protocol was utilized for the formation of Pd cages **9a–c** starting from Pd(dppp)OTf₂. Just as with the Pt cages, when 0.5 equiv of Pd(dppp)OTf₂ was added to a 5 mM solution of cavitant **1** in CD₂Cl₂/CD₃NO₂, hemicage **7** was formed. Due to its higher coordination ability, ethynylpyridine sequestered the whole amount of metal complex added and led to the exclusive formation of **7**. The ¹H NMR spectrum showed the characteristic downfield

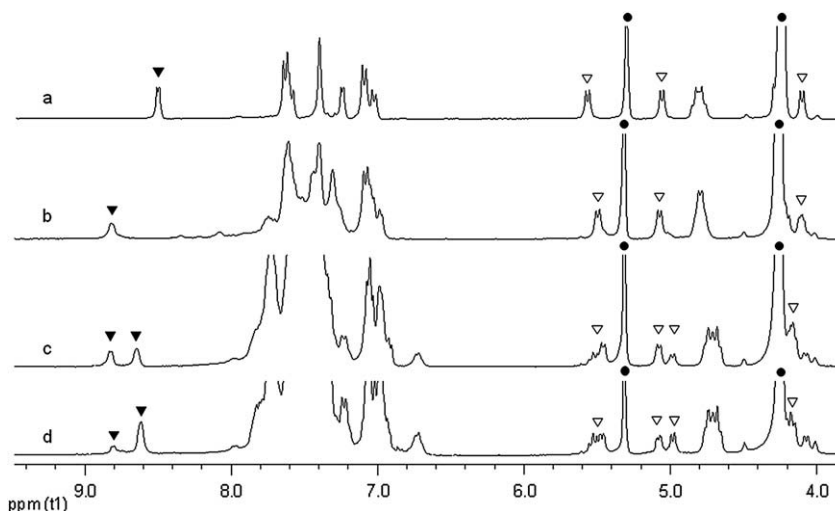


Figure 2. ¹H NMR (300 MHz, 400 μL CD₂Cl₂ and 100 μL CD₃NO₂) spectra of (a) 5 mM cavitant **1**, (b) 5 mM cavitant **1** and 0.5 equiv Pt(dppp)OTf₂, (c) 5 mM cavitant **1** and 2 equiv Pt(dppp)OTf₂, (d) 5 mM cavitant **1** and 2 equiv Pt(dppp)OTf₂ after 48 h. \blacktriangledown ethynylpyridine α -H protons, \triangledown H_{in} and H_{out} methylene bridges protons, \bullet residual solvent peaks.

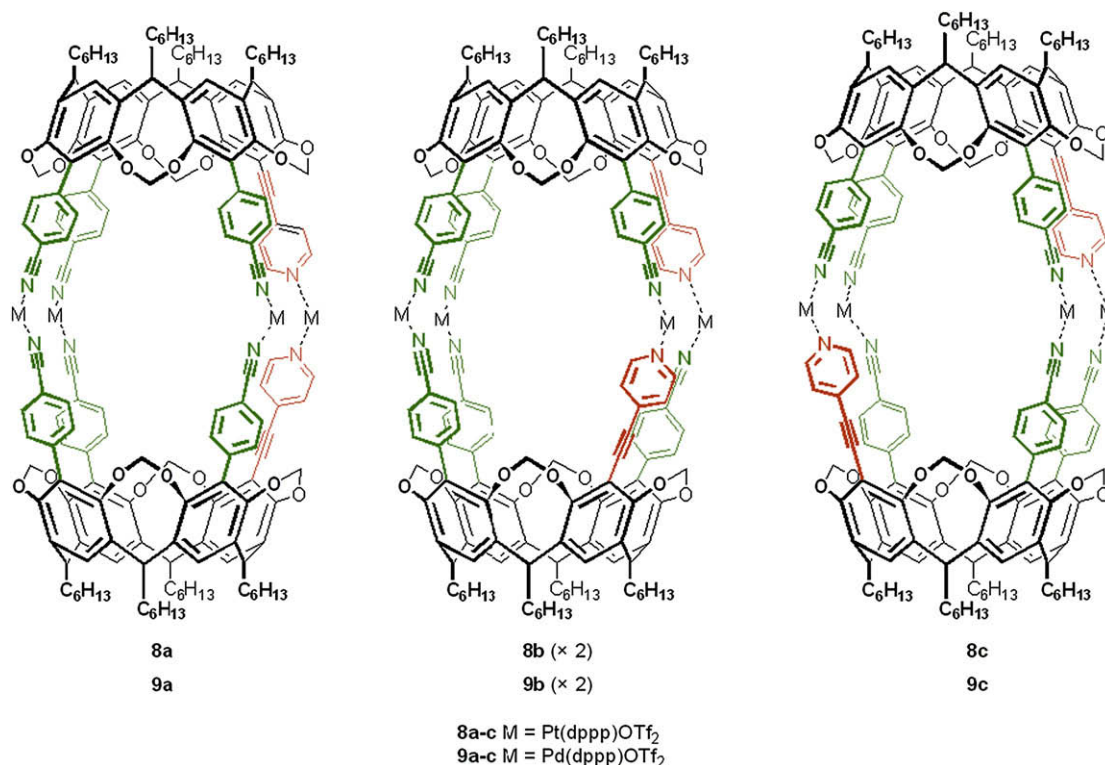


Figure 3. Isomeric coordination cages **8a–c** and **9a–c**.

shift of the peak corresponding to the α -H of the ethynylpyridine ($\Delta\delta = \delta_{\text{hemicage}} - \delta_{\text{free cavitand}} = 0.26$ ppm, from 8.51 to 8.77 ppm). In addition, the H_{out} and H_{in} signals of the methylene bridges adjacent to the ethynylpyridine shifted upfield from 5.60 to 5.49 ppm and from 4.12 to 4.08 ppm (Fig. 4). The ^{31}P NMR signal shifted upfield from 17.26 to 6.14 ppm ($\Delta\delta = \delta_{\text{hemicage}} - \delta_{\text{free Pd metal complex}} = 11.12$ ppm).

After the addition of 1.5 further equivalents of metal complex, two signals for the α -H of the ethynylpyridine were observed at

8.81 and 8.59 ppm, as was the splitting of the H_{in} and H_{out} signals of the methylene bridges. The intensity of the two signals reached a ratio of 1:3 after ca. 48 h (Fig. 4c). Two of the six ^{31}P signals showed the $^2J_{\text{P-P}} = 25$ Hz, which is characteristic for the desymmetrization of the dppp signal in EtPy–CNPh systems.⁸ The diagnostic M^{2+} ion of coordination cages was observed via ESI MS at 2760.1 m/z (Fig. 5). Those data confirmed the formation of three isomeric cages, as previously reported for the Pt experiment.

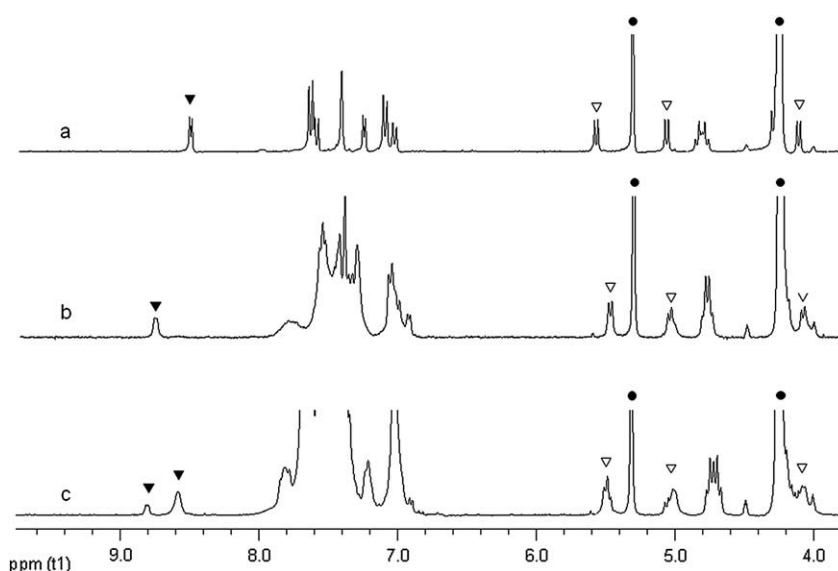


Figure 4. ^1H NMR (300 MHz, 400 μL CD_2Cl_2 and 100 μL CD_3NO_2) spectra of (a) 5 mM cavitand **1**, (b) 5 mM cavitand **1** and 0.5 equiv $\text{Pd}(\text{dppp})\text{OTf}_2$, (c) 5 mM cavitand **1** and 2 equiv $\text{Pd}(\text{dppp})\text{OTf}_2$ after 48 h. ▼ ethynylpyridine α -H protons, ▽ H_{in} and H_{out} methylene bridges protons, ● residual solvent peaks.

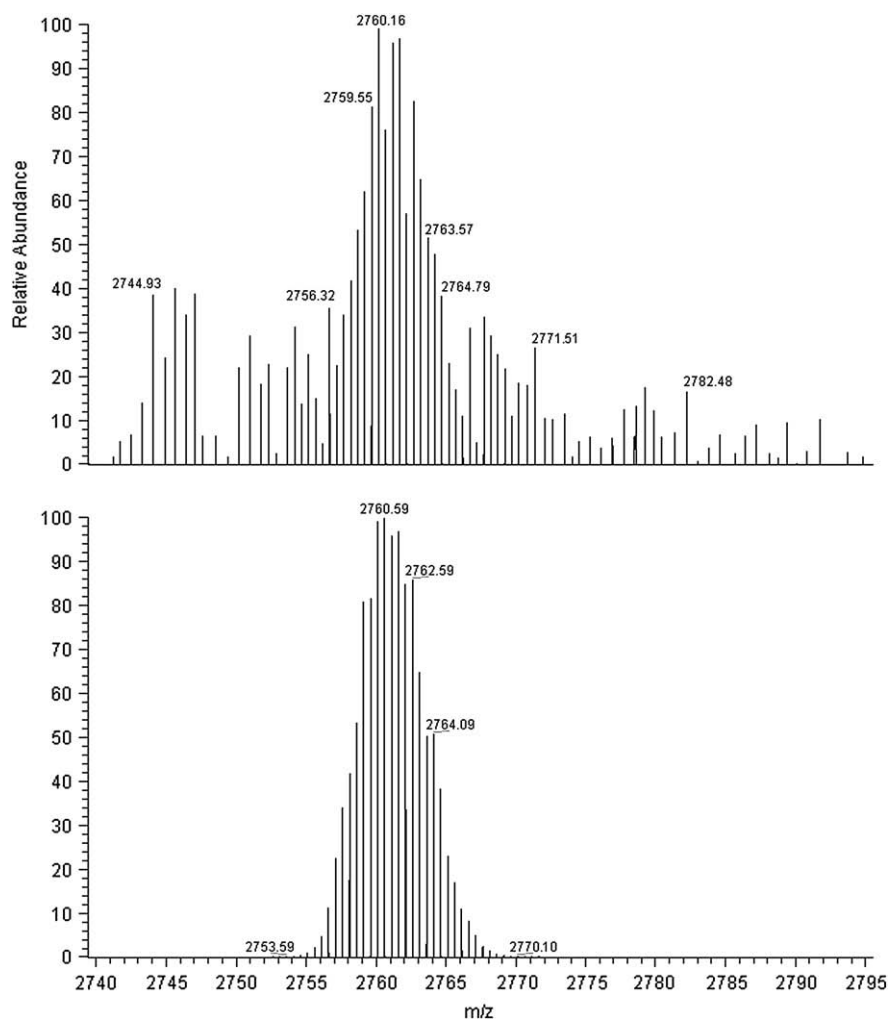


Figure 5. Selected region of the experimental (top) and calculated (bottom) ESI MS spectrum of $\text{CD}_2\text{Cl}_2/\text{CD}_3\text{NO}_2$ solution of cage **9** showing $[\text{M}-2\text{CF}_3\text{SO}_3]^{2+}$ signal at m/z 2760.1.

The different coordination ability of the ligands in **1** could only be exploited for the first step of the self-assembly protocol, leading to homocages **6** and **7**. Further addition of the same metal led to ligand scrambling during subsequent cage closure,

regardless of the metal used. We can conclude that, in itself, the presence of different ligands at the upper rim of the cavitand is not sufficient to drive self-assembly toward the formation of a single molecular cage. Therefore, an additional strategy was

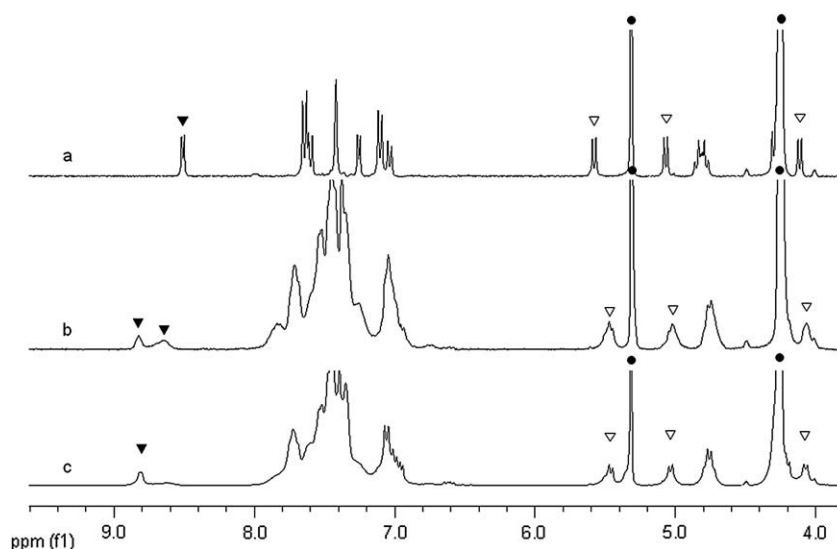


Figure 6. ^1H NMR (300 MHz, 400 μL CD_2Cl_2 and 100 μL CD_3NO_2) spectra of (a) 5 mM cavitand **1**, (b) 5 mM cavitand **1**, 0.5 equiv $\text{Pt}(\text{dppp})\text{OTf}_2$, and 1.5 equiv $\text{Pd}(\text{dppp})\text{OTf}_2$, (c) 5 mM cavitand **1**, 0.5 equiv $\text{Pt}(\text{dppp})\text{OTf}_2$, and 1.5 equiv $\text{Pd}(\text{dppp})\text{OTf}_2$ after one week. ▼ ethynylpyridine α -H protons, ▽ H_{in} and H_{out} methylene bridges protons, ● residual solvent peaks.

devised, involving two different metal centers, to obtain selectively a single cage.

2.4. Self-assembly of heteronuclear cage 10

Addition of 1.5 equiv of Pd(dppp)OTf₂ to a solution of Pt-hemicage **6** led to the exclusive formation of the heterocage **10**. Only one signal for the α -H protons of ethynylpyridine groups and two signals for H_{in} and H_{out}, respectively, were observed in the ¹H NMR spectrum.

Moreover, α -H protons of the ethynylpyridine and H_{in} signals were shifted slightly upfield with respect to hemicage **6** due to the complete closure of the cage ($\Delta\delta=\delta_{\text{cage}}-\delta_{\text{hemicage}}=0.06$ ppm for ethynylpyridine group and $\Delta\delta=\delta_{\text{cage}}-\delta_{\text{hemicage}}=0.05$ ppm for H_{in}). ³¹P NMR exhibited three peaks at –15.48 (EtPy–Pt–PyEt), 11.82 (PhCN–Pd–CNPh), and 15.36 ppm (PhCN–Pd–CNPh) in a 1:2:1 ratio, consistent with the structure of **10**. The presence of the M²⁺ ion in the ESI MS at $m/z=2803.5$ confirmed the formation of the heteronuclear cage. The absence of the M²⁺ ions corresponding to **8** and **9** excluded their presence in solution.

The thermodynamic versus kinetic stability of cage **10** was determined by using a one-pot procedure. Cavitand **1** was reacted with a mixture of Pd(dppp)OTf₂ and Pt(dppp)OTf₂ in a 3:1 ratio in the standard CD₂Cl₂/CD₃NO₂ solution. Initially, two peaks corresponding to the α -H protons of the ethynylpyridine appeared at 8.82 and 8.64 ppm, as did broad signals corresponding to H_{in} and H_{out}, suggesting the formation of a mixture of different cages (Fig. 6b). Within several hours, however, the 8.64 ppm signal disappeared, and the broad H_{in} and H_{out} signals evolved into four doublets at 5.47, 5.05, 4.22 (partially obscured by residual nitromethane solvent signal), and 4.08 ppm. The ¹H NMR spectrum remained unchanged after one week (Fig. 6c). These results indicate the initial formation of several isomeric cages (kinetic products), which interconvert into cage **10** (the thermodynamic product) over time. ¹H and ³¹P NMR confirmed a complete transformation of the isomeric cages into structure **10**.

3. Conclusion

The exclusive formation of heteronuclear coordination cage **10** demonstrates the versatility of this type of self-assembly procedure. The design of the appropriate tetradentate cavitand ligand is the key element in driving the self-assembly toward the formation of the desired product. In the specific case of the heteronuclear coordination cages reported here, it is crucial to differentiate the type, number, and position of the ligands, to reach the correct metal/ligand cross-reactivity. A single ligand substitution with respect to the parent tetrabenzonitrile cavitand¹⁰ is sufficient to shift completely the outcome of the self-assembly protocol from homonuclear to heteronuclear cages. For the same reason, cavitand **1** is unfit for homocage self-assembly, as it leads to the formation of a set of isomeric cages. Efforts to extend this strategy to the self-assembly of large cage networks¹⁶ are underway.

4. Experimental

4.1. General

Reagents and solvents were purchased as reagent grade and used without further purification. Analytical TLC was performed on Merck silica gel 60 F₂₅₄ precoated plates. Column chromatography was performed using silica gel (Merck 70–230 mesh). ¹H NMR spectra were recorded at 300 MHz on a Bruker AC 300 Avance spectrometer with solvent peaks as reference. ³¹P NMR spectra were recorded at 162 MHz, on a Bruker 400 spectrometer. Mass spectra were measured either on a Helwett–Packard 3395

Waters 74 spectrometer or on a LTQ-linear ion trap mass spectrometer (Thermo Fisher Corp.) equipped with an electrospray source.

4.2. Tetraiodo-resorcinarene (3)

To a solution of 0.496 g of resorcinarene **1** (6.02×10^{-4} mol) in a 1:1 mixture of water and diethyl ether (16 mL), 0.202 g of NaHCO₃ (2.41×10^{-4} mol), and 0.614 g of I₂ (2.41×10^{-4} mol) were added. The solution was stirred overnight at room temperature. Following Buchner filtration, the precipitate was washed with cold ethanol. The pure product was collected as white solid (Yield 36%). ¹H NMR (acetone-*d*₆, 300 MHz) δ =8.16 (s, 8H, ArOH), 7.65 (s, 4H, ArH), 4.43 (t, 4H, ArCH, *J*=8.6 Hz), 2.29 (m, 8H, ArCHCH₂), 1.24 (m, 32H, CH₂CH₂CH₂CH₂CH₂CH₃), 0.85 (t, 12H, CH₂CH₃, *J*=7.4 Hz); ESI MS (m/z): 1327 [M][–] [M=C₅₂H₆₈I₄O₈].

4.3. Tetraiodo-cavitand (4)

Compound **1** (0.593 g, 4.46×10^{-4} mol) was dissolved in dry DMF (8 mL) in a dry Schlenk tube. To the solution were added 1.208 mL of CH₂ClBr (1.78×10^{-2} mol) and 0.493 g of K₂CO₃ (3.57×10^{-3} mol). The mixture was stirred at 85 °C for 3 h. After neutralization with HCl 2%, a precipitate formed; following Buchner filtration, the resulting solid was the pure product (Yield 88%). ¹H NMR (CDCl₃, 300 MHz) δ =7.05 (s, 4H, ArH), 5.96 (d, 4H, OCH_{in}H_{out}O, *J*₂=8.2 Hz), 4.84 (t, 4H, ArCH, *J*=9.0 Hz), 4.30 (d, 4H, OCH_{in}H_{out}O, *J*₂=8.2 Hz), 2.18 (m, 8H, ArCHCH₂), 1.31 (m, 32H, CH₂CH₂CH₂CH₂CH₂CH₃), 0.89 (t, 12H, CH₂CH₃, *J*=7.4 Hz); ESI MS (m/z): 1399 [M+Na]⁺ [M=C₅₆H₆₈I₄O₈].

4.4. Monoethynylpyridine-cavitand (5)

Dry Et₃N (10 mL) was degassed in a dry flask for 30 min; 0.5 g of **2** (3.63×10^{-4} mol), 0.084 g of ethynylpyridinehydrochloride (6.25×10^{-4} mol), 0.0102 g of Pd(PPh₃)₂Cl₂ (1.45×10^{-5} mol), 0.0051 g of CuI (3.5×10^{-5} mol), and 0.0057 g of PPh₃ (2.2×10^{-5} mol) were added and the mixture was stirred for 1 h at 60 °C and for 48 h at 90 °C. After cooling to room temperature, CHCl₃ was added and the crude product was washed with water and extracted with CHCl₃. The pure product was obtained by purification with silica gel flash chromatography with CH₂Cl₂/AcOEt (95:5) as eluent (Yield 35%). ¹H NMR (CDCl₃, 300 MHz) δ =8.60 (d, 2H, PyH_o, *J*=6.0 Hz), 7.30 (d, 2H, PyH_m, *J*=6.0 Hz), 7.11 (s, 1H, ArH), 7.08 (s, 1H, ArH), 7.06 (s, 1H, ArH), 5.95 (m, 4H, OCH_{in}H_{out}O), 4.84 (m, 4H, ArCH), 4.48 (d, 2H, OCH_{in}H_{out}O, *J*₂=8.1 Hz), 4.29 (d, 2H, OCH_{in}H_{out}O, *J*₂=8.2 Hz), 2.21 (m, 8H, ArCHCH₂), 1.28 (m, 40H, CH₂CH₂CH₂CH₂CH₂CH₃), 0.88 (t, 12H, CH₂CH₃, *J*=7.2 Hz); ESI MS (m/z): 1352.7 [MH]⁺ [M=C₆₃H₇₂I₃NO₈].

4.5. Monoethynylpyridine-tribenzonitrile cavitand (1)

To a solution of 0.1088 g of **5** (7.45×10^{-5} mol) in 10 mL of dioxane 0.0157 g of Pd(PPh₃)₂Cl₂ (2.24×10^{-5} mol), 0.208 g of 4-(cyanophenyl)boronic acid pinacol ester, (9.07×10^{-4} mol), 0.057 g of AsPh₃ (1.86×10^{-4} mol), and 0.4748 g of Cs₂CO₃ previously dissolved in 0.25 mL of water were added. The mixture was stirred under Argon for 40 h at 110 °C. The solution was cooled at room temperature and concentrated under vacuum. Cavitand **1** was obtained as white solid by precipitation with diethylether in 36% yield. ¹H NMR (CDCl₃, 300 MHz) δ =8.51 (d, 2H, PyH_o, *J*=6.0 Hz), 7.65 (d, 4H, NCArH_o, *J*=9.1 Hz), 7.59 (d, 2H, NCArH_o, *J*=9.1 Hz), 7.29 (s, 4H, ArH), 7.21 (d, 2H, PyH_m, *J*=6.0 Hz), 7.15 (d, 4H, NCArH_m, *J*=9.1 Hz), 7.09 (d, 2H, NCArH_m, *J*=9.1 Hz), 5.60 (d, 2H, OCH_{in}H_{out}O, *J*₂=7.8 Hz), 5.17 (d, 2H, OCH_{in}H_{out}O, *J*₂=7.7 Hz), 4.80 (m, 4H, ArCH), 4.38 (d, 2H, OCH_{in}H_{out}O, *J*₂=7.8 Hz), 4.12 (d, 2H, OCH_{in}H_{out}O, *J*₂=7.7 Hz), 2.30 (m,

8H, ArCHCH₂), 1.22 (m, 32H, CH₂CH₂CH₂CH₂CH₂CH₃), 0.90 (t, 12H, CH₂CH₃, *J*=7.3 Hz); ESI MS (*m/z*): 1278.6 [MH]⁺, [M=C₈₄H₈₄N₄O₈].

4.6. Stepwise self-assembly of Pt-hemicage (6) and Pt cage (8)

To a solution of 3.2 mg of **1** (5.0×10^{-3} M) in CD₂Cl₂ (0.4 mL) and CD₃NO₂ (0.1 mL) in the NMR tube 1.1 mg of Pt(dppp)OTf₂ was added to give hemicage **6** and ¹H NMR and ³¹P NMR spectra were recorded. ¹H NMR (CD₂Cl₂+CD₃NO₂, 300 MHz): δ=8.82 (d, 4H, PyHo), 7.76–6.98 (m, 48H, PPh₂+NCArH_o+PyH_m+NCArH_m), 5.49 (d, 4H, OCH_{in}H_{out}O), 5.07 (d, 4H, OCH_{in}H_{out}O), 4.80–4.78 (m, 8H, ArCH), 4.20 (d, 4H, OCH_{in}H_{out}O partially under residual solvent peak), 4.10 (d, 4H, OCH_{in}H_{out}O), 2.29 (m, 16H, ArCHCH₂), 1.29 (m, 64H, CH₂CH₂CH₂CH₂CH₂CH₃), 0.90 (br t, 24H, CH₂CH₃); ³¹P NMR (CD₂Cl₂+CD₃NO₂, 162 MHz): –15.60 ppm (*J*_{P–Pt}=3033 Hz).

An additional 3.4 mg of Pt(dppp)OTf₂ was added to same solution and ¹H NMR and ³¹P NMR spectra were recorded again. ¹H NMR (CD₂Cl₂+CD₃NO₂, 300 MHz): δ=8.81 (d, 4H, PyHo), 8.61 (d, 12H, PyHo), 7.82–6.98 (m, 416H, PPh₂+NCArH_m+NCArH_o), 6.92 (d, 4H, PyH_m), 6.72 (d, 12H, PyH_m), 5.55–5.42 (m, 16H, OCH_{in}H_{out}O), 5.08 (d, 8H, OCH_{in}H_{out}O), 4.98 (d, 8H, OCH_{in}H_{out}O), 4.75–4.65 (m, 32H, ArCH), 4.26–4.22 (m, 16H, OCH_{in}H_{out}O), 4.23 (d, 8H, OCH_{in}H_{out}O partially under residual solvent peak), 4.18 (d, 16H, OCH_{in}H_{out}O), 2.90 (m, 64H, dppp), 2.75 (m, 32H, dppp), 2.29 (m, 64H, ArCHCH₂), 1.29 (m, 256H, CH₂CH₂CH₂CH₂CH₂CH₃), 0.90 (br t, 96H, CH₂CH₃); ³¹P NMR (CD₂Cl₂+CD₃NO₂, 162 MHz): –15.60, –10.02 (*J*_{P–Pt}=3444 Hz).

ESI MS (*m/z*): 2938.2 [(M–2OTf)]²⁺, [M=C₂₈₄H₂₇₂F₂₄N₈O₄₀–P₈Pt₈S₈].

4.7. Stepwise self-assembly of Pd hemicage (7) and Pd cage (9)

To a solution of 3.1 mg of **1** (4.85×10^{-3} M) in CD₂Cl₂ (0.4 mL) and CD₃NO₂ (0.1 mL) in the NMR tube 1 mg of Pd(dppp)OTf₂ was added to give hemicage **7** and ¹H NMR and ³¹P NMR spectra were recorded. ¹H NMR (CD₂Cl₂+CD₃NO₂, 300 MHz): δ=8.77 (d, 4H, PyHo), 7.67–7.30 (m, 32H, PPh₂+NCArH_o), 7.06 (d, 12H, NCArH_m), 6.94 (d, 4H, PyH_m), 5.49 (d, 4H, OCH_{in}H_{out}O), 5.05 (d, 4H, OCH_{in}H_{out}O), 4.81–4.75 (m, 8H, ArCH), 4.22–4.19 (m, 4H, OCH_{in}H_{out}O, partially under residual solvent peak), 4.08 (d, 4H, OCH_{in}H_{out}O), 3.12–2.91 (dppp signals), 2.32 (m, 16H, ArCHCH₂), 1.29 (m, 64H, CH₂CH₂CH₂CH₂CH₂CH₃), 0.87 (br t, 24H, CH₂CH₃); ³¹P NMR (CD₂Cl₂+CD₃NO₂, 162 MHz): δ=6.14 ppm.

An additional 2.9 mg of Pd(dppp)OTf₂ was added to same solution and ¹H NMR and ³¹P NMR spectra were recorded again. ¹H NMR (CD₂Cl₂+CD₃NO₂, 300 MHz): δ=8.81 (d, 4H, PyHo), 8.59 (d, 12H, PyHo), 7.84–6.89 (m, PPh₂+NCArH_m+NCArH_o+PyH_m), 5.51–5.46 (m, 16H, OCH_{in}H_{out}O), 5.07–4.99 (m, 16H, OCH_{in}H_{out}O), 4.77–4.66 (m, 32H, ArCH), 4.19–4.07 (m, 32H, OCH_{in}H_{out}O partially under residual solvent peak), 2.90–2.75 (m, three signals of dppp), 2.29 (m, 64H, ArCHCH₂), 1.40–1.29 (m, 256H, CH₂CH₂CH₂CH₂CH₂CH₃), 0.87 (br t, 96H, CH₂CH₃); ³¹P NMR (CD₂Cl₂+CD₃NO₂, 162 MHz): δ=15.77, 12.41, 11.50 (d, ²*J*_{P–P}=25 Hz), 10.90 (d, ²*J*_{P–P}=25 Hz), 6.14, 4.91 ppm.

ESI MS (*m/z*): 2760.16 [(M–2OTf)]²⁺, [M=C₂₈₄H₂₇₂F₂₄N₈O₄₀–P₈Pd₈S₈].

4.8. Self-assembly of heteronuclear cage (10)

4.8.1. Stepwise procedure

To a solution of 3.2 mg of **1** (5×10^{-3} M) in CD₂Cl₂ (0.5 mL) in the NMR tube 1.1 mg of Pt(dppp)OTf₂ was added to form Pt-hemicage **6**. Pd(dppp)OTf₂ (3 mg) was added to same solution and ¹H NMR

and ³¹P NMR spectra were recorded. ¹H NMR (CD₂Cl₂, 300 MHz): δ=8.89 (d, 4H, PyHo), 7.73–7.30 (m, 92H, PPh₂+NCArH_o), 7.13–7.07 (m, 12H, NCArH_m), 6.98 (d, 4H, PyH_m), 5.47 (d, 4H, OCH_{in}H_{out}O), 5.05 (d, 4H, OCH_{in}H_{out}O), 4.80–4.72 (m, 8H, ArCH), 4.28–4.26 (m, 4H, OCH_{in}H_{out}O), 4.08 (d, 4H, OCH_{in}H_{out}O), 3.24 (m, 8H, dppp), 2.90 (m, 8H, dppp), 2.30 (m, 24H, dppp+ArCHCH₂), 1.42–1.34 (m, 64H, CH₂CH₂CH₂CH₂CH₂CH₃), 0.93 (br t, 24H, CH₂CH₃); ³¹P NMR (CD₂Cl₂, 162 MHz): δ=15.36, 11.82, –15.48 (*J*_{P–Pt}=3189 Hz).

4.8.2. One-pot procedure

To a solution of 3.5 mg of **1** (5.4×10^{-3} M) in CD₂Cl₂ (0.4 mL) and CD₃NO₂ (0.1 mL) in the NMR tube 1.25 mg of Pt(dppp)OTf₂, and 3.3 mg of Pd(dppp)OTf₂ were added. ¹H NMR and ³¹P NMR spectra were recorded. ¹H NMR (CD₂Cl₂+CD₃NO₂, 300 MHz): δ=8.82 (d, 4H, PyHo), 7.72–7.25 (m, 92H, PPh₂+NCArH_o), 7.07–6.94 (m, 16H, PyH_m+NCArH_m), 5.46 (d, 4H, OCH_{in}H_{out}O), 5.03 (d, 4H, OCH_{in}H_{out}O), 4.79–4.74 (m, 8H, ArCH), 4.20 (d, 4H, OCH_{in}H_{out}O partially under residual solvent peak), 4.07 (d, 4H, OCH_{in}H_{out}O), 3.23–2.83 (m, dppp), 2.30 (m, 16H, ArCHCH₂), 1.40–1.29 (m, 64H, CH₂CH₂CH₂CH₂CH₂CH₃), 0.87 (br t, 24H, CH₂CH₃); ³¹P NMR (CD₂Cl₂+CD₃NO₂, 162 MHz): δ=15.84, 12.35, –15.07 (*J*_{P–Pt}=3075 Hz).

ESI MS (*m/z*): 2803.51 [(M–2OTf)]²⁺, [M=C₂₈₄H₂₇₂F₂₄N₈O₄₀–Pd₃P₈PtS₈].

Acknowledgements

This work was supported by the EU through NoE MAGMANet (3-NMP 515767-2). The instrumental facilities at the Centro Interfacoltà di Misure G. Casnati of the University of Parma were utilized.

References and notes

- Pirondini, L.; Dalcanele, E. In *Modern Supramolecular Chemistry*, Diedrich, F., Stang, P.J., Tykwinski, R.R., Eds.; Wiley-VCH: Weinheim, 2008; Chapter 7, pp 233–276.
- (a) Harrison, R. G.; Burrows, J. L.; Hansen, L. D. *Chem.—Eur. J.* **2005**, *11*, 2881–2888; (b) Haino, T.; Kobayashi, M.; Fukazawa, Y. *Chem.—Eur. J.* **2006**, *12*, 3310–3319.
- (a) Caulder, D. L.; Powers, K. N.; Parac, T. N.; Raymond, K. N. *Angew. Chem., Int. Ed.* **1998**, *37*, 1840–1843; (b) Fochi, F.; Jacopozi, P.; Wegelius, E.; Rissanen, K.; Cozzini, P.; Marastoni, E.; Fisciuro, E.; Manini, P.; Fokkens, R.; Dalcanele, E. *J. Am. Chem. Soc.* **2001**, *123*, 7539–7552; (c) Fujita, M.; Yoshizawa, M. In *Modern Supramolecular Chemistry*, Diedrich, F., Stang, P.J., Tykwinski, R.R., Eds.; Wiley-VCH: Weinheim, 2008; Chapter 8, pp 277–313.
- (a) Chen, J.; Köner, S.; Craig, S. L.; Rudkevich, D. M.; Rebek, J., Jr. *Nature* **2002**, *415*, 385–386; (b) Yoshizawa, M.; Sato, N.; Fujita, M. *Chem. Lett.* **2005**, *34*, 1392–1393.
- Koblentz, T. S.; Dekker, H. L.; de Koster, C. G.; van Leeuwen, P. W. N. M.; Reek, J. N. H. *Chem. Commun.* **2006**, 1700–1702.
- Rudkevich, D. M. *Angew. Chem., Int. Ed.* **2004**, *43*, 558–571.
- (a) Warmuth, R. *Eur. J. Org. Chem.* **2001**, 423–437; (b) Yoshizawa, M.; Kusukawa, T.; Fujita, M.; Yamaguchi, K. *J. Am. Chem. Soc.* **2000**, *122*, 6311–6312.
- Yamanaka, M.; Yamada, Y.; Sei, Y.; Yamaguchi, K.; Kobayashi, K. *J. Am. Chem. Soc.* **2006**, *128*, 1531–1539.
- For the self-assembly of heterocages on surfaces, see: (a) Menozzi, E.; Pinalli, R.; Speets, E. A.; Ravoo, B. J.; Dalcanele, E.; Reinhoudt, D. N. *Chem.—Eur. J.* **2004**, *10*, 2199–2206; (b) Busi, M.; Laurenti, M.; Condorelli, G. G.; Motta, A.; Favazza, M.; Fragalà, I. L.; Montalti, M.; Prodi, L.; Dalcanele, E. *Chem.—Eur. J.* **2007**, *13*, 6891–6898.
- Cuminetti, N.; Ebbing, M. H. K.; Prados, P.; de Mendoza, J.; Dalcanele, E. *Tetrahedron Lett.* **2001**, *42*, 527–530.
- Pinalli, R.; Cristini, V.; Sottili, V.; Geremia, S.; Campagnolo, M.; Caneschi, A.; Dalcanele, E. *J. Am. Chem. Soc.* **2004**, *126*, 6516–6517.
- Tunstad, L. M.; Tucker, J. A.; Dalcanele, E.; Weiser, J.; Bryant, J. A.; Sherman, C. J.; Helgeson, R. C.; Knobler, C. B.; Cram, D. J. *Org. Chem.* **1989**, *54*, 1305–1312.
- Tanaka, Y.; Sasada, A.; Fujita, Y. *Proceedings of 9th International Conference on Calixarene Chemistry*, **2007**; p 96.
- Román, E.; Peinador, C.; Mendoza, S.; Kaifer, A. E. *J. Org. Chem.* **1999**, *64*, 2577–2578.
- Zuccaccia, D.; Pirondini, L.; Pinalli, R.; Dalcanele, E.; Macchioni, A. *J. Am. Chem. Soc.* **2005**, *127*, 7025–7032.
- Menozzi, E.; Busi, M.; Massera, C.; Ugozzoli, F.; Zuccaccia, D.; Macchioni, A.; Dalcanele, E. *J. Org. Chem.* **2006**, *71*, 2617–2624.